

AD-A114 063

ROCKWELL INTERNATIONAL THOUSAND OAKS CA MICROELECTR--ETC F/G 20/2
RESEARCH ON THE CRYSTAL GROWTH AND DIELECTRIC PROPERTIES OF HIG--ETC(U)
APR 82 R R NEURGAONKAR, W W HO, W F HALL N00014-81-C-0463
MRDC*1091.2AR NL

UNCLASSIFIED

1 of 1
PDA
10001

END
DATE
FILMED
5-82
DTIC

AD A114063

(12)

10

April, 1982

MRDC41091.2AR

RESEARCH ON THE CRYSTAL GROWTH AND DIELECTRIC
PROPERTIES OF HIGH PERMITTIVITY FERROELECTRIC MATERIALS


Annual Report
For Period 05/15/81 through 02/28/82
Contract No. N00014-81-C-0463

General Order No. 41091

Prepared for:

Scientific Officer
Director Metallurgy and Ceramics Program
Material Sciences Division
Office of Naval Research
800 N. Quincy St.
Arlington, Virginia 22217

Prepared by:


R. R. Neurgaonkar

Principal Investigator *

Assisted by:

* (W.W. Ho and W. F. Hall)

DTIC
ELECTE
MAY 3 1982
H

DISTRIBUTION STATEMENT A
Approved for public release;
Distribution Unlimited

DTIC FILE COPY



Rockwell International

Microelectronics Research
and Development Center

82

05

05

000

UNCLASSIFIED

SECURITY CLASSIFICATION OF THIS PAGE (When Data Entered)

REPORT DOCUMENTATION PAGE		READ INSTRUCTIONS BEFORE COMPLETING FORM
1. REPORT NUMBER	2. GOVT ACCESSION NO.	3. RECIPIENT'S CATALOG NUMBER
	AD A114063	
4. TITLE (and Subtitle) Research on the Crystal Growth and Dielectric Properties of High Permittivity Ferroelectric Materials.		5. TYPE OF REPORT & PERIOD COVERED Annual Technical Report 05/15/81 through 02/28/82
7. AUTHOR(s) R. R. Neugaonkar		6. PERFORMING ORG. REPORT NUMBER MRDC41091.2AR
9. PERFORMING ORGANIZATION NAME AND ADDRESS Rockwell International MRDC 1049 Camino Dos Rios, Thousand Oaks, CA. 91360		8. CONTRACT OR GRANT NUMBER(s) N00014-81-C-0463
11. CONTROLLING OFFICE NAME AND ADDRESS Office of Naval Research 800 N. Quincy St. Arlington, VA. 22217		10. PROGRAM ELEMENT, PROJECT, TASK AREA & WORK UNIT NUMBERS MRDC41091.2AR
14. MONITORING AGENCY NAME & ADDRESS (if different from Controlling Office)		12. REPORT DATE April, 1982
		13. NUMBER OF PAGES 21
		15. SECURITY CLASS. (of this report) Unclassified
		16a. DECLASSIFICATION/DOWNGRADING SCHEDULE
16. DISTRIBUTION STATEMENT (of this Report) Approved for public release; distribution unlimited.		
17. DISTRIBUTION STATEMENT (of the abstract entered in Block 20, if different from Report)		
18. SUPPLEMENTARY NOTES		
19. KEY WORDS (Continue on reverse side if necessary and identify by block number) Strontium potassium niobate Soft-mode Czochralski growth technique Dielectric relaxation Low frequency dielectric High frequency		
20. ABSTRACT (Continue on reverse side if necessary and identify by block number) Single crystals of $\text{Sr}_{0.2}\text{KNb}_{0.8}\text{O}_{15}$ (SKN), approximately 5-8 mm in diameter and 10-20 mm long, have successfully been grown by the Czochralski technique. The crystal has ferroelectric tetragonal tungsten bronze structure with a curie temperature of about 150°C. The dielectric and electromechanical coupling constants for this crystal have been established: the polar axis		

DD FORM 1 JAN 73 1473

EDITION OF 1 NOV 65 IS OBSOLETE

UNCLASSIFIED

SECURITY CLASSIFICATION OF THIS PAGE (When Data Entered)

UNCLASSIFIED

SECURITY CLASSIFICATION OF THIS PAGE(When Data Entered)

dielectric constant, K_{33}^T exceeds 20,000 at the curie temperature while the coupling constants are $k_{33}^T = 0.52$ and $k_{31}^T = 0.19$, respectively. High frequency dielectric properties of SKN samples were also determined between 90-100 GHz. These measurements indicated that the bulk of the polar axis permittivity has relaxed below 90 GHz, implying that the low frequency dielectric response is not soft-mode controlled.

SECURITY CLASSIFICATION OF THIS PAGE(When Data Entered)



TABLE OF CONTENTS

	<u>Page</u>
1. Progress Summary	01
2. Introduction.....	02
3. Materials Development.....	03
3.1 Tungsten Bronze Family.....	03
3.2 The System $\text{SrNb}_2\text{O}_6\text{-KNbO}_3$	03
3.3 Bulk Single Crystal Growth Procedure.....	05
4. Low Frequency Characterization.....	11
4.1 Poling Procedure.....	11
4.2 Dielectric Data.....	12
5. High Frequency Characterization.....	17
6. Future Plans.....	20
7. References.....	21



Accession For	
NTIS GRA&I	<input checked="" type="checkbox"/>
DTIC TAB	<input type="checkbox"/>
Unannounced	<input type="checkbox"/>
Justification	
By	
Distribution/	
Availability Codes	
Dist	Avail and/or Special
A	



LIST OF FIGURES

1. Projection of structure of tetragonal tungsten bronze parallel to (001).
2. The SrNb_2O_6 - KNbO_3 pseudo-binary join. * = DTA solidus and liquidus temperature and x= quench runs.
3. Shows a Schematic diagram of a typical Czochralski crystal growth unit.
4. Shows a typical SKN single crystal grown along the (001) direction.
5. Temperature dependence of dielectric constant (K_{33}) for SKN crystal.
6. Temperature dependence of dielectric constant (K_{33}) for SKN crystal (logarithmic scale).
7. Temperature dependence of dielectric loss for SKN crystal at three frequencies: 1, 10 and 100 KHz.
8. Typical microwave apparatus used to determine the dielectric properties of a sample (SKN) mounted in a waveguide.
9. Dielectric properties of SKN single crystal samples from 90-100 GHz.
Top: Real (ϵ') and imaginary (ϵ'') permittivity along a-axis.
Bottom: Real (ϵ') and imaginary (ϵ'') permittivity along c-axis.



LIST OF TABLES

1. Properties of three $\text{Sr}_2\text{KNb}_5\text{O}_{15}$ compositions.
2. Physical properties of various tungsten bronze crystals.



1.0 PROGRESS SUMMARY

During the first nine months of this program, phase equilibria studies on the proposed system $\text{SrNb}_2\text{O}_6\text{-KNbO}_3$ have been initiated to establish the congruent melting composition in this system. Although further work is necessary to establish complete phase equilibria data, it has been shown in the present study that the compositions close to the $\text{Sr}_2\text{KNb}_5\text{O}_{15}$ region (about 74 mole% SrNb_2O_6) are suitable for single crystal growth work. The Czochralski growth technique has now been established and SKN single crystals of this composition (74 mole% SrNb_2O_6) as large as 5-7 mm in diameter and 10-20 mm long have successfully been grown. This is a major and important achievement in the present work. Although the SKN single crystals thus obtained are sufficient to initiate high frequency dielectric measurements, efforts are underway to develop this technique to produce large size crystals, approximately 1 to 1.5cm in diameter. Low frequency dielectric measurements on these crystals show a well defined peak in K_{33} at 150°C in excess of 20,000 for a frequency of 1 KH_z . At room temperature, K_{33} is approximately 180 and shows no frequency dependence up to 100 KH_z . The loss tangent was found to be roughly 0.02 independent of frequency and temperature below 130°C .

Substantial dispersion has been observed in the dielectric properties of SKN single crystal at frequencies between 90 and 100 GH_z . The polar axis permittivity has fallen to approximately 50, compared to its low frequency value of 180, while the polar axis loss tangent is large ($\tan \delta_{33} \sim 0.25$). It appears that the bulk of the permittivity is not contributed by the soft mode, which in this system should be found above 10^{12}Hz .



2.0 INTRODUCTION

The microwave properties of high dielectric constant materials such as ferroelectrics, relaxo-ferroelectrics, and antiferroelectrics generally show complex behavior that has been variously interpreted in terms of soft lattice modes, soft relaxation processes in the lattice, and microscopic domain dynamics. In many cases, these interpretations predict significant effects associated with the transition between paraelectric and ferro- or dielectric properties, to occur in the frequency range from 2×10^{10} to 10^{12} Hz. However, there is at present a nearly total lack of dielectric measurements in this range.

The proposed program is intended to provide this basic data on the temperature, frequency, and electric field dependence of the susceptibility above 20 GHz for suitably chosen structural classes of materials. Selected members of these classes are to be grown and thoroughly characterized by standard methods, and interpretations of the observed properties are to be derived in terms of Devonshire free energy models for each class.



3.0 MATERIAL DEVELOPMENT

3.1 Tungsten Bronze Family

The tungsten bronze structure family is one of the most extensive, versatile, and potentially useful families of oxygen octahedron based ferroelectrics. This structural family embraces more than 100 individual end member compositions, and continuous solid solution is possible between many of these end members (1-3). The tetragonal tungsten bronze unit cell of the paraelectric prototypic structure is shown in Fig. 1 in projection on the (001) plane (4). It consists basically of a complex array of corner sharing distorted MO_6 octahedra arranged in such a manner that there are three different types of interstice in between. Thus there are five structurally different cation sites labeled A, B, C and two different octahedral sites labeled M'M" (5). Bronzes can then be designated with compositions such as $A_4B_2M_{10}O_{30}$ or $A_4B_2C_4M_{10}O_{30}$ depending on the valence of the substituent ABC and M cations which occupy the 15, 12, 9 and 6 fold coordinated sites. It is this structural complexity which will accommodate a wide range of cation substitutions that is responsible for the versatility of the ferroelectric properties in the bronze family, but also for the major practical problem which has heretofore limited their utility.

3.2 The System $SrNb_{2-6}O_{15}$ - $KNbO_3$

Ferroelectric alkali-alkaline earth niobates with tetragonal tungsten bronze related structure show considerable promise for dielectric and nonlinear electro-optic applications. Among the materials of interest, $Sr_2KNb_5O_{15}$ and $Ba_2KNb_5O_{15}$ exhibit excellent dielectric properties and a room temperature electro-optic effect nearly an order of magnitude greater than that of $LiNbO_3$. Efficient second harmonic generation of YAG:Nd³⁺ laser radiation has been demonstrated in these types of materials. As emphasized in our research program, the single crystal growth work on the $Sr_2KNb_5O_{15}$

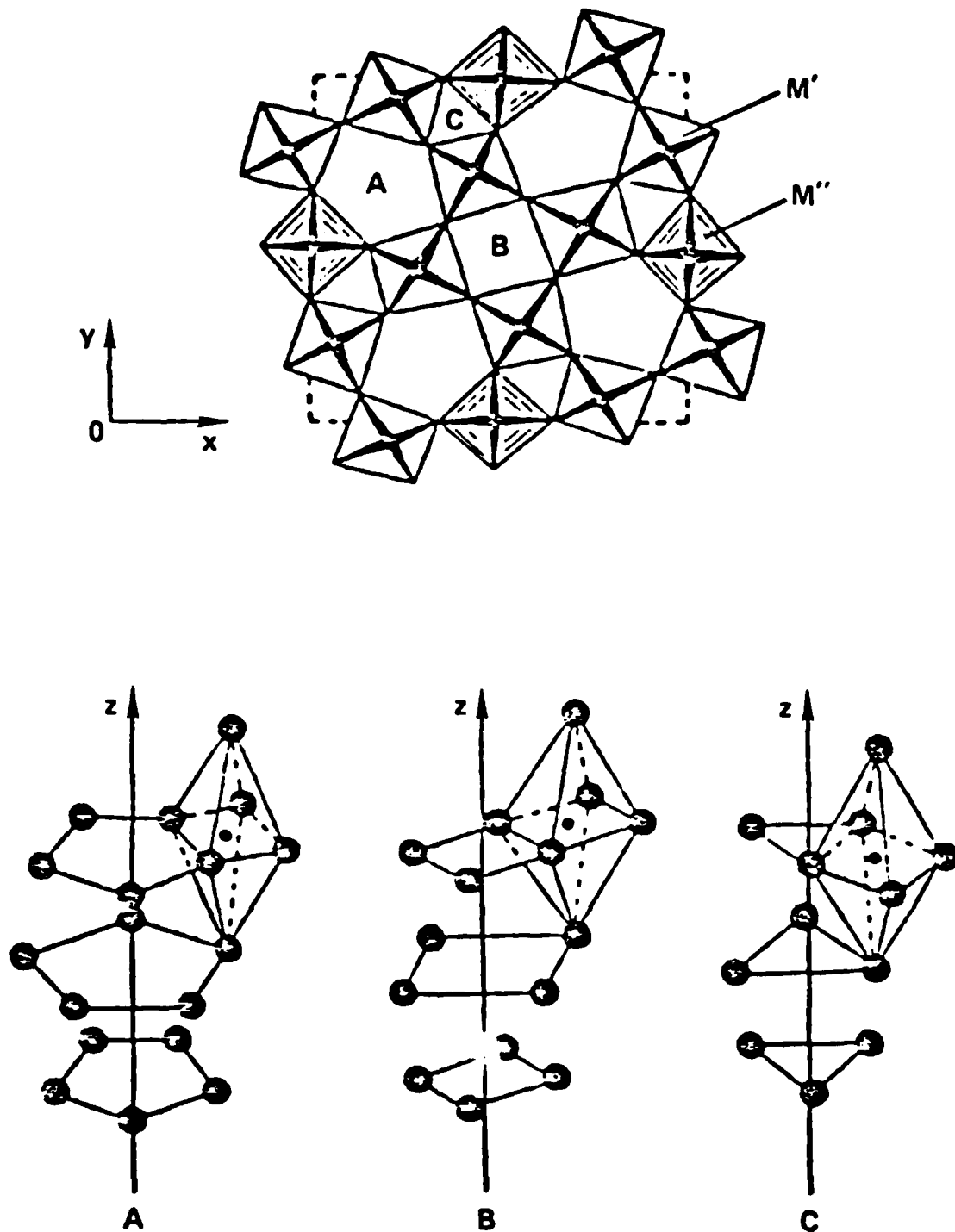


Fig. 1. Projection of structure of tetragonal tungsten bronze parallel to $[001]$.



composition has already been initiated to determine its low and high frequency dielectric properties. The SKN composition exists on the pseudo-binary system $\text{SrNb}_2\text{O}_6\text{-KNbO}_3$ and this composition melts around 1475°C . It has also been reported that the Sr:K ratio (i.e., $\text{SrNb}_2\text{O}_6\text{:KNbO}_3$) can be varied while still maintaining the tetragonal tungsten bronze structure even though neither of the end members has this structure. Other examples of this behavior can be found in the BaNb_2O_6 ^(6,7) and related systems. Table IV summarizes the changes in dielectric constant with changes in the Sr:K ratio ⁽⁸⁾.

Phase equilibria studies of the $\text{SrNb}_2\text{O}_6\text{-KNbO}_3$ system have been reported by Scott et al. ⁽⁹⁾ and Ainger et al. ⁽¹⁰⁾. Figure 2 shows a phase relation in the pseudo-binary system $\text{SrNb}_2\text{O}_6\text{-KNbO}_3$ system (after Scott et. al.). Their results are not in complete agreement. According to Scott et. al., the congruent melting composition of 77% SrNb_2O_6 is slightly off from the $\text{Sr}_2\text{KNb}_5\text{O}_{15}$ region, while Ainger et al. claimed that the potassium deficient composition $\text{K}_{.5}\text{Sr}_{2.5}\text{Nb}_5\text{O}_{15}$ (84% SrNb_2O_6) is the congruent melting composition on this system. In order to confirm these results before the single crystal growth of SKN was developed in the present program, a few compositions around the $\text{Sr}_2\text{KNb}_5\text{O}_{15}$ region were examined using the X-ray diffraction and DTA techniques. The results of this investigation are not complete, but it has been shown that the compositions close to 74% SrNb_2O_6 are suitable for the single crystal growth of SKN; and hence this composition has been selected in the proposed work. The phase equilibria work is in progress and based on these results changes will be made in the melt compositions, if necessary.

3.3 Bulk Single Crystal Growth Procedure

Single crystals of SKN were grown by the Czochralski technique from both iridium and platinum crucibles with successful results. Fig. 3 shows a schematic diagram of a typical Czochralski crystal grown unit. In the case of iridium crucibles, argon pressure had to be used to prevent excessive loss of iridium, and as-grown crystals were found to be purple or coal black in color. However, the color changed to deep yellow when



TABLE I *

Crystal Composition Mole %			P_s at 22°C $\mu\text{C cm}^{-2}$		ϵ' at 22°C		T_c (°C)
K ₂ O	SrO	Nb ₂ O ₅	Poled	Unpoled	Poled	Unpoled	
11	40	49	29	0	490	900	155
5	44	51	25	0	820	1300	138
4	42	54	24	0	1000	1500	120

PROPERTIES OF THREE $\text{Sr}_2\text{KNb}_5\text{O}_{15}$ COMPOSITIONS

*Data taken from Ref. 10 (Ainger et al.)



the crystals were annealed in oxygen over 1000°C. Oxygen pressure was directly employed when crystals were pulled from platinum crucibles; crystals thus obtained are pale yellow in color. Since the lattice mismatch between SKN and $\text{Sr}_{.61}\text{Ba}_{.39}\text{Nb}_2\text{O}_6$ (SBN) bronze composition is minimal, the SBN single crystals were directly used as seed material in the present growth work. This proved to be very successful and SKN single crystals as large as 5-7 mm in diameter and 10-20 mm long have been grown. Although further improvements are necessary, this is a major and significant achievement in the proposed research work. Optimum conditions used are as follows:

Pulling Rate:	5-8 mm/hr
Rotation Rate:	15-25 rpm
Growth Direction:	Along the (001) direction
Growth Temperature:	1475°C

The single crystal growth of SKN has also been studied and reported by Geiss et al. ⁽¹¹⁾ and Ainger et al. ⁽¹⁰⁾, and the results of this investigation are in close agreement with their work. Figure 4 shows a typical SKN single crystal grown along the (001) direction. Although the SKN crystals obtained in the present work are sufficiently large to initiate high frequency dielectric measurements, the present Czochralski technique is being improved to develop large size crystals, approximately 1 to 1.5 cm in diameter. Based on our ongoing work on tungsten bronze family single crystals, the growth of large sized crystals depends strongly on the ability to control the diameter of crystal and the thermal gradient in the crystal near the solid-liquid interface. Since this work has only been in progress for the last several months, all the experimental parameters have not yet been established. It is therefore reasonable to conclude that with further improvement in experimental conditions, specifically in the thermal gradient, it should be possible to grow larger diameter SKN crystals.

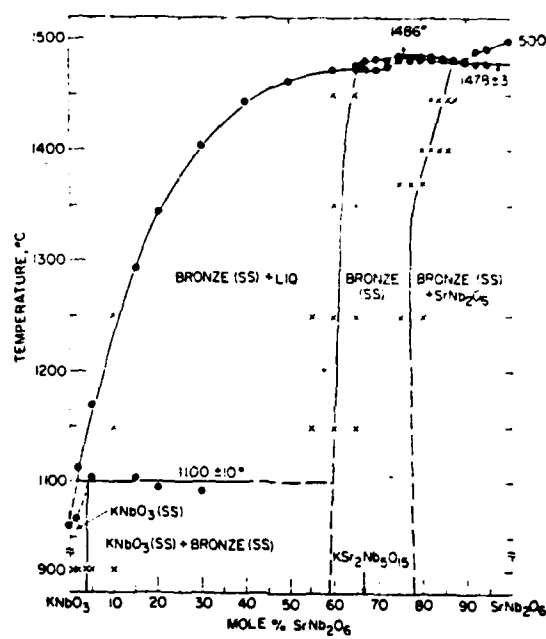


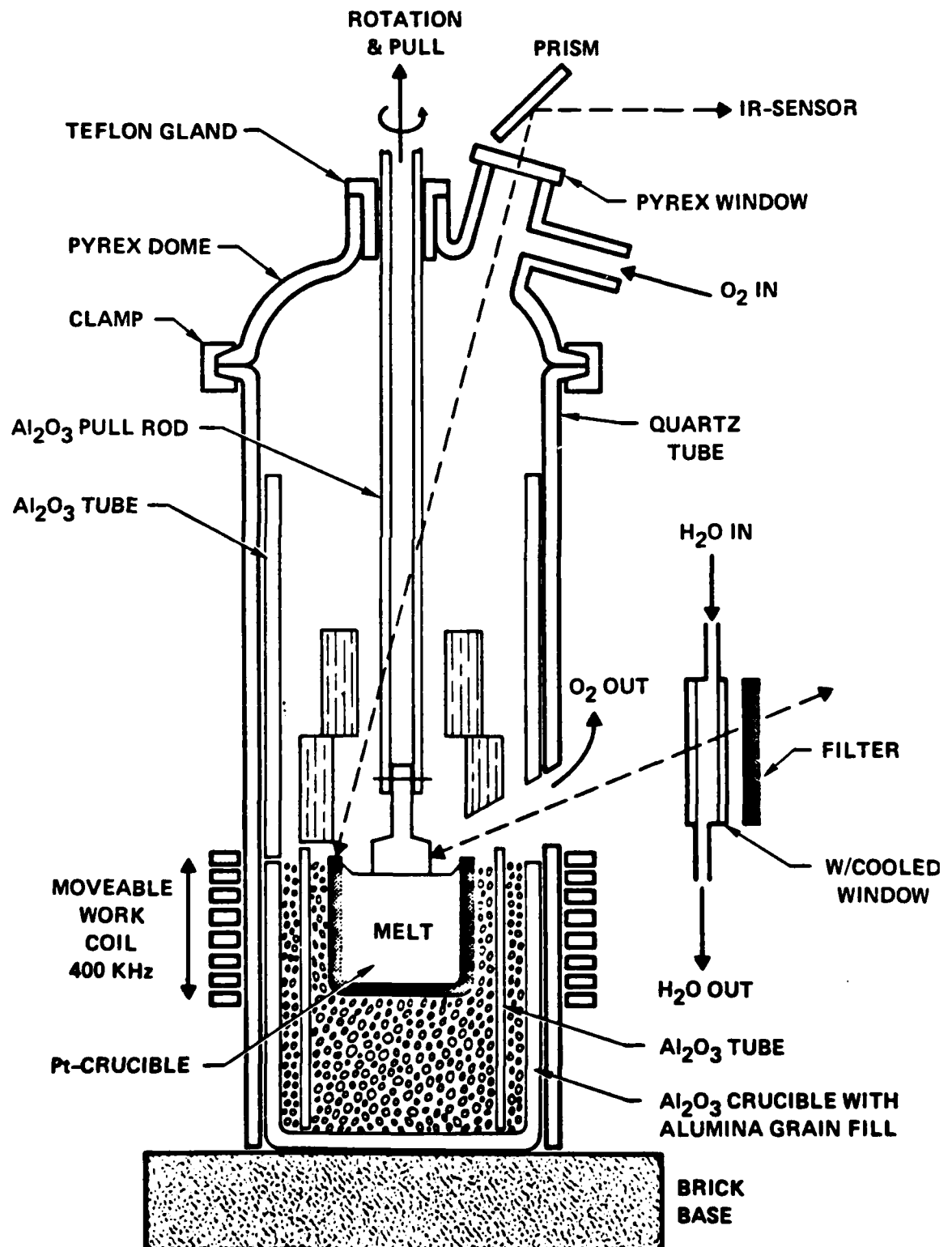
Figure 2.

The KNbO_3 - SrNb_2O_6 join. ●=DTA solidus and liquidus temperatures and x = quench runs.



FIGURE 3.

Schematic diagram of a typical Czochralski crystal growth unit.





Rockwell International

MRDC41091.2AR

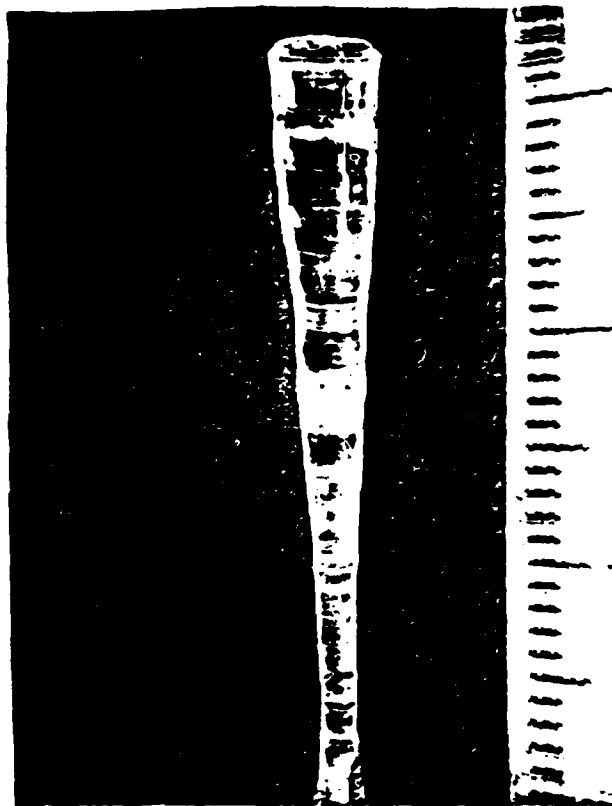


Figure 4 shows a typical SKN single crystal grown along the (001) direction.



4.0

LOW FREQUENCY CHARACTERIZATION

Optically, the SKN single crystals appear to be of excellent quality and are clear and transparent. Crystals grown along the c-axis are usually well faceted, which is quite exceptional for the Czochralski grown crystals. X-ray diffraction studies show that the crystal habits are based on 24 faces of four prism: (110), (120), (100) and (130). In the present case the SKN crystal showed several such facets, but they were not as well defined as seen in other bronze single crystal such as $\text{Sr}_{0.6}\text{Ba}_{0.4}\text{Nb}_2\text{O}_6$. Crystals showed room temperature tungsten bronze tetragonal structure and, according to structural refinements for this family, this composition belongs to the point group 4 mm. The lattice constants measurements for the ceramic and single crystal samples of the 74% composition SKN ($74\% \text{SrNb}_2\text{O}_6 + 24\% \text{KNbO}_3$) gave values of $a = 12.458 \text{ \AA}$ and $c = 3.944 \text{ \AA}$, which are in close agreement with the value $a = 12.470 \text{ \AA}$ and $c = 3.942 \text{ \AA}$ reported by Geiss et al (11) for a 76% composition.

4.1 Poling Procedure

To obtain optimum ferroelectric characteristics such as electro-mechanical coupling constants or piezoelectric constants, it is important that the crystal be single domain. Therefore, it is necessary in the present work to prepare single domain SKN single crystal for evaluation of their ferroelectric characteristics. Based on our temperature dependent dielectric measurements on the SKN single crystals grown in the present work, the ferroelectric phase transition temperature (T_c) occurs around 150°C ; this information is important in controlling the poling temperature. The procedure for poling used here consists of heating the grown SKN single crystal to about 10°C over the curie temperature, with d c field around 6 KV/cm along the c-axis. The poling temperature was slowly reduced to room temperature while the dc field was maintained and and this proved to be successful to prepare single domain SKN crystal. The poling field was established by measuring the electromechanical coupling constant k_{33} using a resonance technique, which is defined as:



$$k^2 = \frac{f_A^2 - f_R^2}{f_A^2}, \text{ Where, } f_R = \text{Resonance Frequency}$$
$$f_A = \text{Antiresonance frequency}$$

The coupling constants k_{33} and k_{31} were established and they were 0.52 and 0.12 respectively. These values were of significantly lower orders when the poling field was below 6KV/cm.

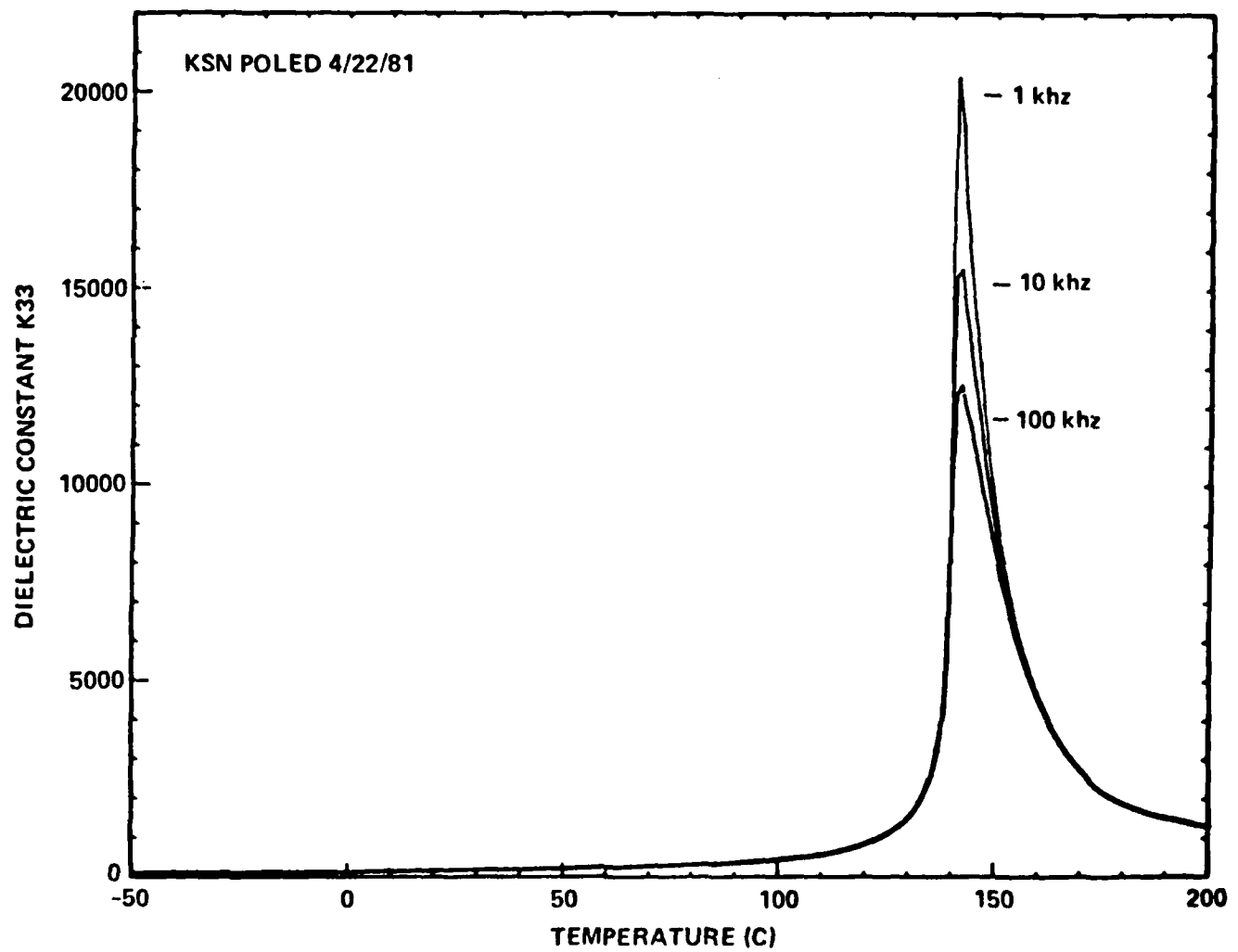
4.2 Dielectric Data

Low-frequency dielectric measurements were initiated on the SKN single crystals and these measurements are very interesting. This has been accomplished by measuring the temperature dependence of capacitance over the temperature range -50° to 200°C . A crystal used for these measurements was approximately 1 mm in thickness; aluminum electrodes were deposited on both sides. The dielectric measurements were performed using three different frequencies, i.e., 1, 10 and 100 KHz and the results of these experiments have been summarized in Figures 5 and 6. As can be seen from Figure 5, at room temperature K_{33} is 2×10^2 and peaks above 10^4 at the Curie temperature. The values of K_{33} will vary to some extent with amount of K and Sr in the crystal. Above the transition temperature a Curie law $K_{33} = C/(T-T_c)$ is found to hold for the crystals measured with C in the range $2-4 \times 10^{20}\text{C}$. Figure 6 shows the dielectric loss for the present SKN single crystals. Figure 7 shows temperature dependence of dielectric loss for SKN crystal at three frequencies: 1, 10 and 100 KHz.

Table 2 summarizes physical constants for the SKN and other important bronze single crystals, e.g. $\text{Sr}_{.6}\text{Ba}_{.4}\text{Nb}_2\text{O}_6$ and $\text{K}_3\text{Li}_2\text{Nb}_5\text{O}_{15}$. The results of the low frequency measurements clearly indicate that the SKN crystal possesses excellent-dielectric properties and should prove to be a useful candidate to explore the high frequency (in min-wave range) dielectric properties and their fundamental characteristics. In the following sections, results on the high frequency dielectric properties of this crystal are presented.



FIGURE 5



Temperature dependence of dielectric constant (K_{33}) for SKN crystal.

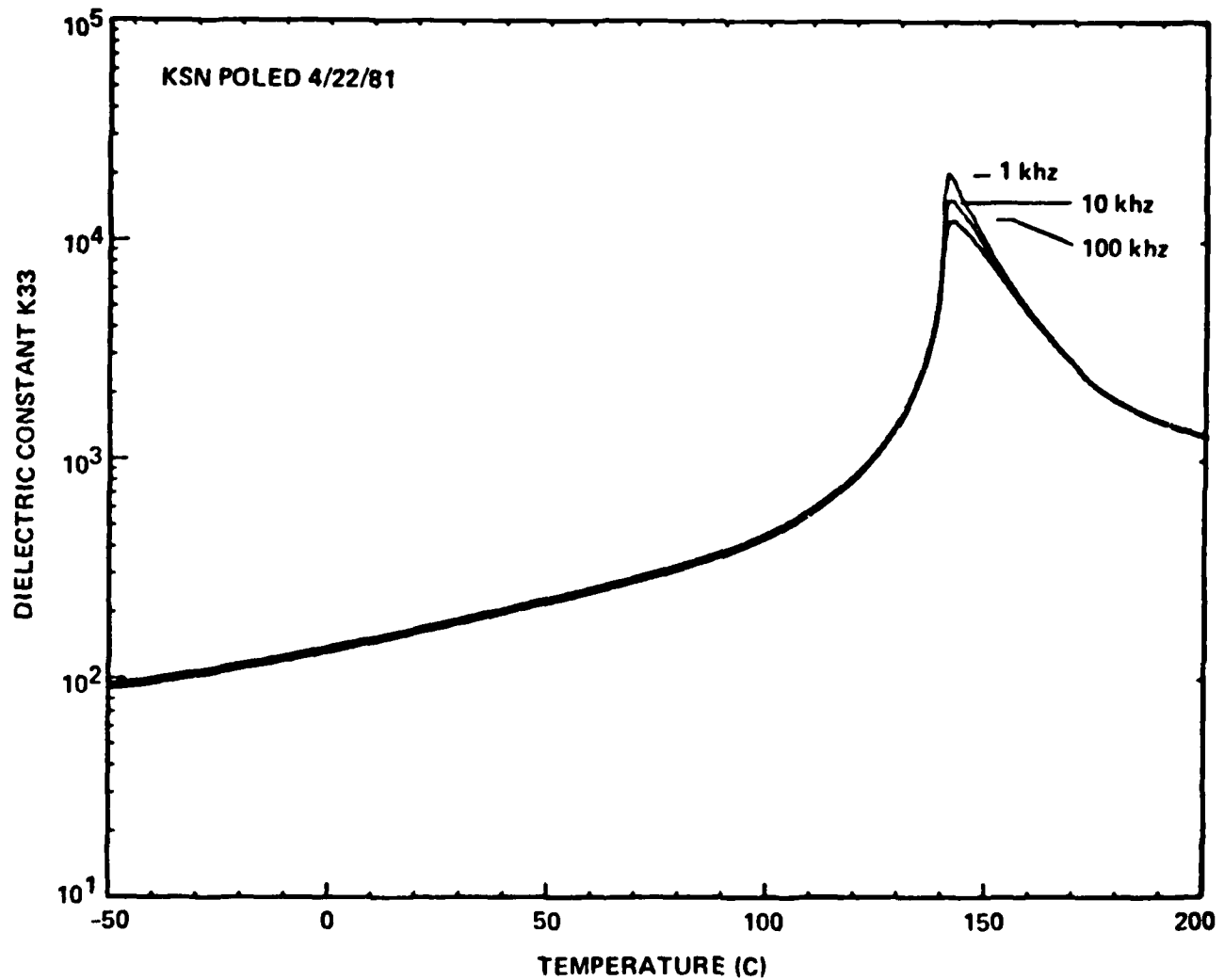
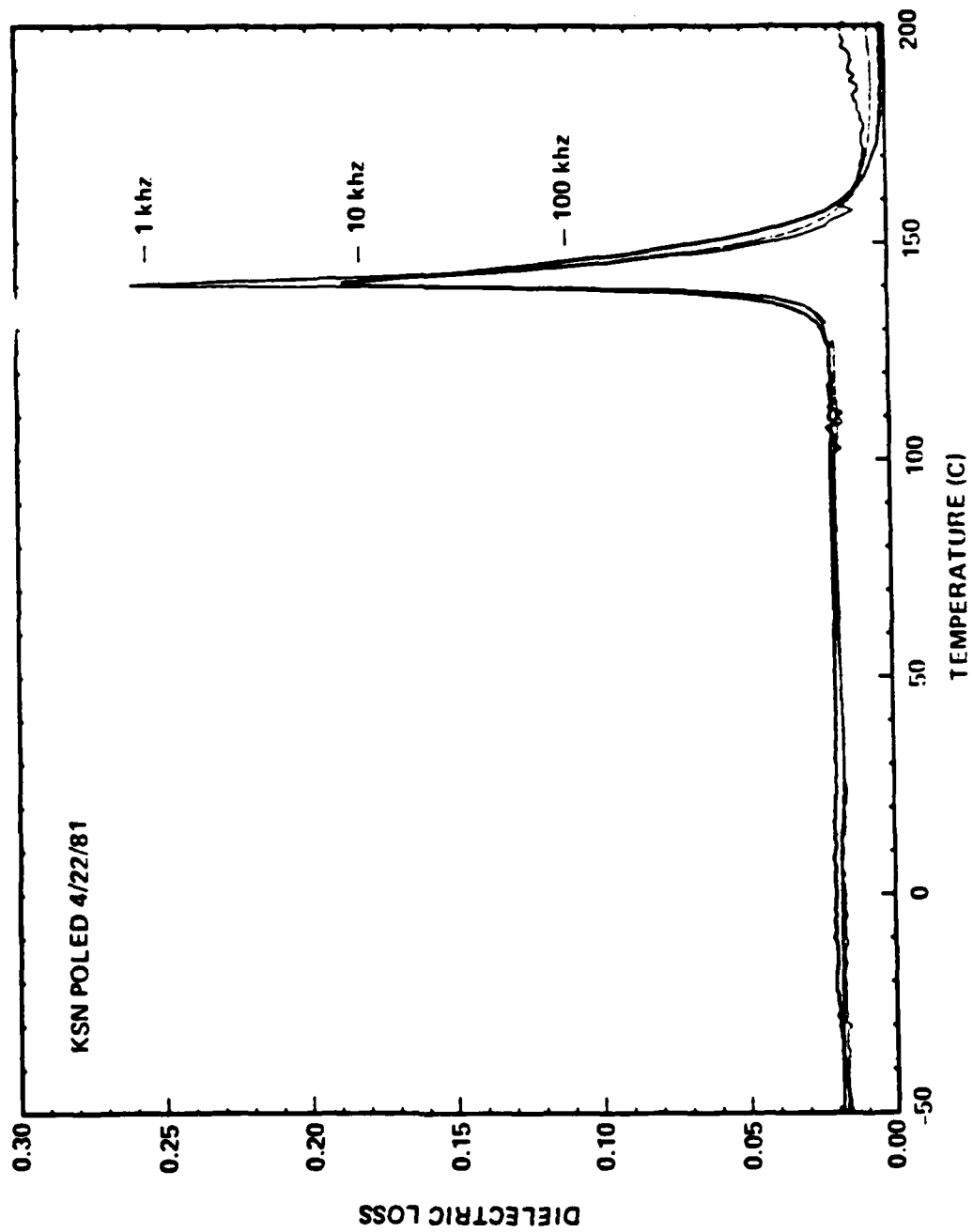


Figure 6. Temperature dependence of dielectric constant (K_{33}) for SKN crystal (logarithmic scale).



FIGURE 7.



Temperature dependence of dielectric loss of SKN crystals at three frequencies:
1, 10 and 100 KHz.

PHYSICAL PROPERTIES OF VARIOUS T. B. CRYSTALS

TABLE 2.

Property	SKN	SBN:60	KLN
Unit Cell	Tetragonal	Tetragonal	Tetragonal
Space Group	4mm	4mm	4mm
Unicell	a=12.47Å	a=12.468Å	a=12.59Å
- - - - -	- - - - -	- - - - -	- - - - -
Facets	Several, less	Well defined	Well defined
- - - - -	defined	24	4
- - - - -	- - - - -	- - - - -	- - - - -
Curie Temperature °C	150°C	72°C	405°C
E ₃₃ at 25°C	200	880	150
E ₃₃ at T _c	20,000	≥ 20,000	~1000
- - - - -	- - - - -	- - - - -	- - - - -
Electromechanical	k ₃₃ =0.52	k ₃₃ =0.47	k ₃₃ =0.54
Coupling Constant	k ₃₁ =0.12	k ₃₁ =0.14	k ₃₁ =0.18
- - - - -	k ₁₅ = -	k ₁₅ =0.13	k ₃₃ =0.35
- - - - -	- - - - -	- - - - -	- - - - -
Piezoelectric Strain	d ₃₃ = -	d ₃₃ = 30	d ₃₃ =57
Constant	d ₃₁ = -	d ₃₁ =130	d ₃₁ =-14
- - - - -	d ₁₅ = -	d ₁₅ = 31	d ₁₅ =68

SBN:60 -----Sr_{.6}Ba_{.4}Nb₂O₆KLN-----K₃Li₂Nb₅O₁₅



5.0 HIGH FREQUENCY CHARACTERIZATION

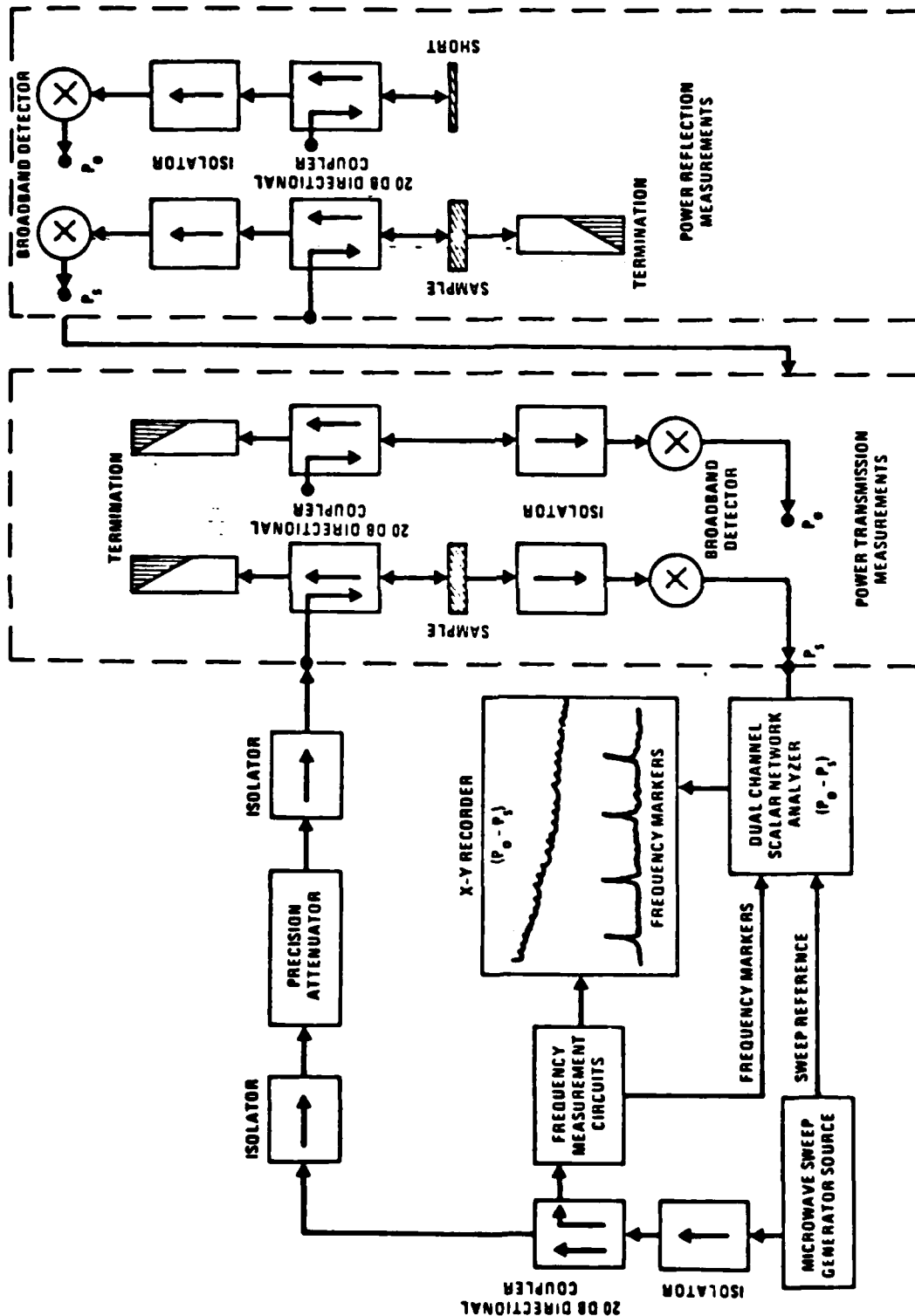
Room-temperature reflection and transmission measurements have been carried out between 90 and 100 GHz on four small single-crystal samples cut from a single boule of SKN and oriented to allow determination of the complex dielectric permittivities parallel and perpendicular to the crystal polar axis. These measurements were made in waveguide, as indicated in Figure 8, with the sample filling the guide cross-section.

The dielectric permittivities derived from these data show a large dispersion, with ϵ'_{33} having fallen to one quarter of its low-frequency value, while ϵ'_{11} in this range of frequencies is about twice ϵ'_{33} . The frequency dependence of these parameters is summarized in Figure 9. along with the dielectric loss ϵ''_{11} and ϵ''_{33} (upper and lower sections of the figure, respectively).

The large decrease observed in ϵ'_{33} from its low-frequency value strongly suggests that the bulk of the polar axis permittivity is not contributed by the soft mode, which is thought to lie above 10^{12} Hz in this temperature range. Rather, mechanisms must be sought having characteristic relaxation at GHz frequencies, such as piezoelectric resonance in microdomains of submicron dimension. Point defects, or perhaps dislocations induced by compositional gradients in the crystal, may act to stabilize such domains against poling. The relatively high observed loss ($\tan \delta_{33} \sim 0.25$, $\tan \delta_{11} \sim 0.13$) and the variation in permittivity between samples from the same boule are also consistent with an extrinsic GHz relaxation mechanism.



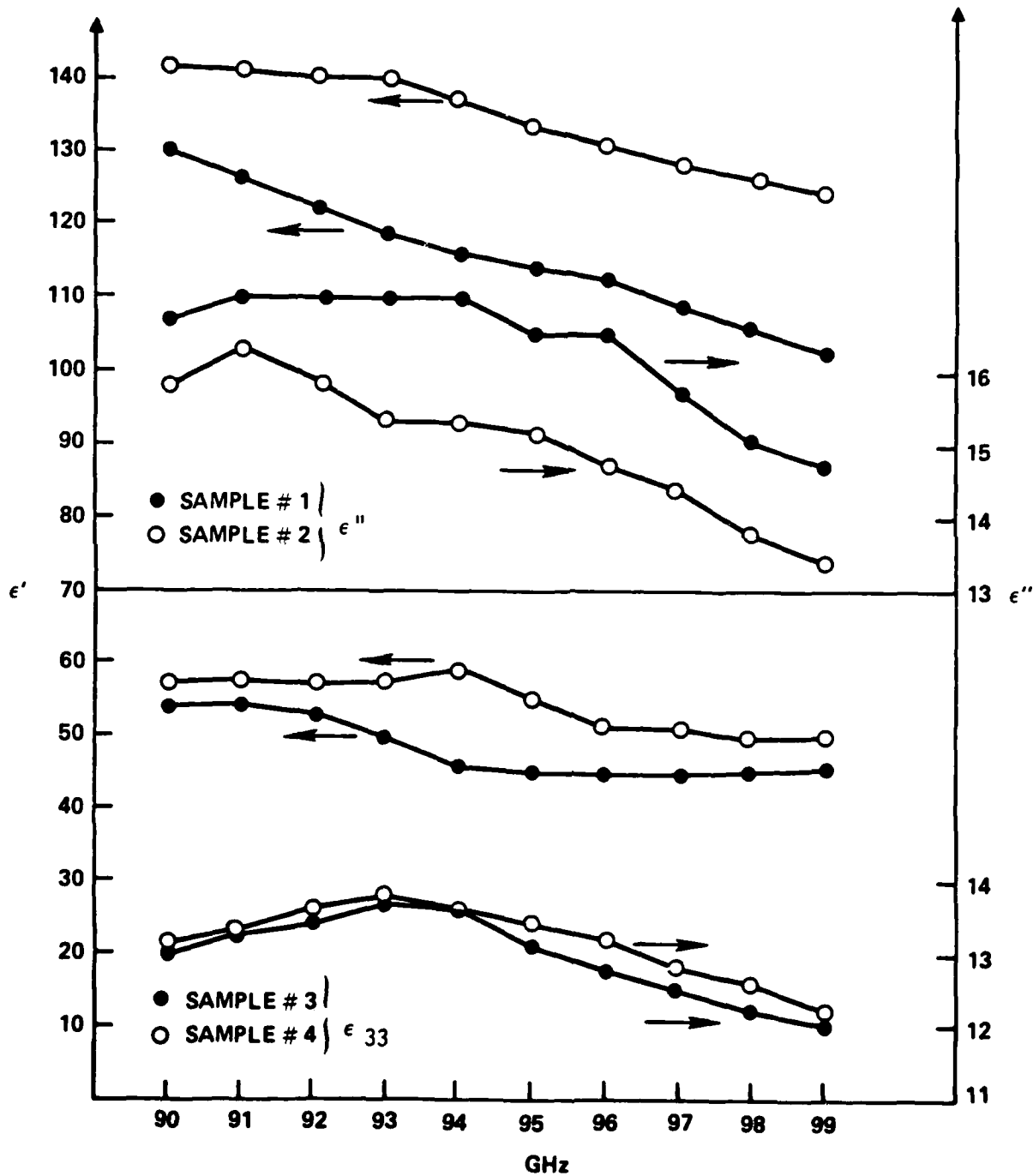
FIGURE 8.



Typical microwave apparatus used to determine the dielectric properties of a sample mounted in a waveguide.



FIGURE 9.



Dielectric properties of SKN single crystal samples for 90-100 GHz.
Top: Real (ϵ') and Imaginary (ϵ'') permittivities along crystal a-axis
Bottom: Real (ϵ') and Imaginary (ϵ'') permittivities along crystal c-axis.



Recently, we have observed similar behavior in strontium barium niobate single crystals between 30 and 40 GHz, measured as part of an ongoing DARPA program to develop millimeter wave phase shifting materials. In one such sample, the polar axis permittivity was approximately 35 over the whole frequency range from 30 to 40 GHz, compared to a low-frequency permittivity of 900. This suggests that the phenomenon we are observing may be generally responsible for the high dc permittivities in the tungsten bronze family.

6.0 FUTURE PLANS

The observation of substantial dispersion in the dielectric properties of SKN and SBN single crystals at millimeter wave frequencies calls for an extension of our studies to include other closely-related ferroelectrics, as well as a more thorough investigation of temperature and frequency dependence in the present system. Presently under consideration are the "stuffed" tungsten bronze $\text{Ba}_{2-x}\text{Sr}_x\text{K}_{1-y}\text{Na}_y\text{Nb}_5\text{O}_{15}$, which has all cation sites occupied and therefore has less tendency toward disorder, and the orthorhombic tungsten bronze $\text{Pb}_2\text{KNb}_5\text{O}_{15}$ (PKN) and $\text{K}_2\text{BiNb}_5\text{O}_{15}$ (KBN), where both a- and c-axis are polar. Comparison of the dielectric dispersion along the polar and non-polar axes in these systems should suggest directions for further exploration of the mechanisms responsible for the observed dielectric properties.



7.0 REFERENCES

1. Landolt-Bornstein, Vol. 3 (1969); Vol 16 a (1980), Ferroelectric and Antiferroelectric Substances, Ed. T. Mitsui, Springer Verlag, New York.
2. J. Ravez, A. Perron Simon, P. Hagenmuller, Ann. Chim., 1:251, (1976).
3. R. R. Neurgaonkar, Semiannual Technical Report No. 2, Contract No. F49620-78-C-0093.
4. P. B. Jamieson, S. C. Abrahams, J. L. Bernstein, J. Chem. Phys., 48:5048 (1968).
5. P. B. Jamieson, S.C. Abrahams, J. L. Bernstein, J. Chem. Phys., 50:4352 (1969).
6. A. A. Ballman and H. Brown, J. Crystal Growth 1, 311, (1967).
7. M. H. Francombe, Acta. Cryst. 13, 131 (1960).
8. R. Clarke and F. W. Ainger, Ferroelectrics, 7, 101, (1974).
9. B. A. Scott, E. A. Geiss, D.F. O'Kane and G. Burns, J. Am. Ceram. Soc. 53, 106 (1970).
10. F. W. Ainger, J. A. Beswick and S. G. Porter, Ferroelectrics, 3, 321, (1972).
11. E. A. Geiss, G. Burns, D. F. O'Kane and A. W. Smith, Appl. Phys. Lett. 11, 233 (1967).

DATE
ILME